IAC-18-D4.3-18

# Disassembly of Near Earth Asteroids by Leveraging Rotational Self-Energy

Andrea Viale[a*]
a.viale.1@research.gla.ac.uk

Colin McInnes[b]
Colin.Mcinnes@glasgow.ac.uk

Matteo Ceriotti[c]
Matteo.Ceriotti@glasgow.ac.uk

*a,b,c*: University of Glasgow, Glasgow G12 8QQ, UK.
* : corresponding author.

**Abstract**

One of the key challenges for future space exploration is to envisage efficient ways to exploit the material resources available in the family of near-Earth asteroids. These resources have been recognised as a potentially lower cost alternative sources of materials to those launched to Earth escape (such as water, metals and liquid propellants). Several studies have investigated the accessibility of these resources, as those asteroids are among the easiest celestial bodies to reach from Earth. These scenarios will require, in particular, the design of efficient methods to lift material from the surface of near-Earth asteroids, for direct exploitation or for partial disassembly. In the latter case this is to increase the exposed surface area of the material, for example to harvest water using solar concentrator technologies. In this paper, an efficient concept is presented to raise material from the surface of a rotating asteroid. Building on the orbital siphon concept it is shown that, by connecting multiple payloads from the surface of an ideal spherical asteroid as an $n$-body tethered system, the centrifugal pull due to the body's spin can overcome the gravitational force on the payloads, eventually allowing the resource payloads to escape. A stream of such payloads can therefore be envisaged to provide a continuous mass flow from the surface of the asteroid into orbit without the need for external work to be done. The paper will use this initial analysis of the mechanics of the problem to investigate the engineering requirements for such a resource extraction system such as tether length, tension and anchoring force requirements, achievable mass flow rates for candidate objects.

## 1. Introduction

Accessing near-Earth asteroid resources represents a fundamental challenge for the future of space exploration. near-Earth asteroids are likely targets for resources which may serve as support for space industrialization. In fact, they could provide a variety of resources such as water, metals and semiconductors, useful for propulsion, manufacturing of space structures, life support, metallurgy and propulsion [1]. Material could be processed both in-situ or in Earth orbit, the optimal choice depending on the asteroid of interest. When in-situ processing is addressed, partial disassembly of the asteroid may be useful to increase the surface-to-volume ratio of the body, thus facilitating processing of water and minerals by sublimation using solar concentrator technologies [2, 3].

Recent interest in asteroid disassembly is shown in [4] where reconfigurable robotic spacecraft with a large surface area are optimezd to move in proximity of the asteroid surface, extract material and then launch it into orbit, where it would be collected by an orbiting resource processing spacecraft.

The work in this paper is motivated by such interest in asteroid disassembly to facilitate resource processing. The analysis has its root in the concept of the *orbital siphon*, devised by Davis and elaborated by McInnes [5]. The idea is to leverage the rotational kinetic energy of a rotating asteroid to deliver a fraction of its mass into orbit, without the need for external work to be done. This can be accomplished by connecting multiple payloads from the surface of an ideal spherical asteroid as an $n$-body tethered system (Fig. 1): the centrifugal pull due to the body's spin can overcome the gravitational force on the payloads, eventually allowing the resource payloads to escape. The requirement of lifting material into bound motion around the asteroid will then pose constraints on the minimum angular velocity of the asteroid and the minimum chain length [6].

Building on the orbital siphon concept, a simple system architecture is proposed which guarantees effective orbital siphon operation. Then, the en-

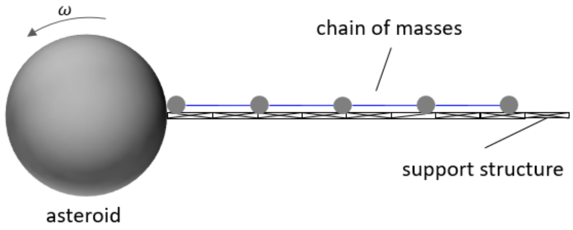


**Figure 1:** Model of radial chain of masses.

gineering requirements for such a system are explored.

The paper is organized as follows. The key elements of the orbital siphon concept are introduced in Sect. 2. Possible candidate objects matching the requirements for the orbital siphon effect to take place are then listed. A preliminary system architecture to keep the chain of masses radial and provide a continuous stream of resources is described in Sect. 3. A simple model of the proposed architecture is developed and analysed in Sect. 4. Section 5 contains the main results and discussion. Conclusions follow in Sects. 6 and 7.

### 2. Orbital Siphon concept

The analytical mechanics of asteroid disassembly using the orbital siphon concept is described in [6]. The main aspects are here noted.

The asteroid is modelled as a spherical body with uniform density, rotating with constant angular velocity. A chain with $n \geq 2$ payload masses (PMs) is attached to the equator and each PM can slide frictionless along a rigid support structure which is assumed to be fixed at the equator of the asteroid (Fig. 1). On each PM, the reaction centripetal force due to asteroid rotation will act as an outward force in the radial direction, while the gravitational force acts in the opposite direction. If the chain is long enough, the overall centrifugal force summed over all the PMs can be larger than the gravitational pull, thus allowing the chain to lift.

This effect can be utilized to provide a continuous stream of resource payloads from the surface of the asteroid into orbit (*orbital siphon effect*): new payloads are connected to the bottom of the chain while end payloads are removed and released into orbit, without the need for external work to be done.

It has been shown [6] that the specific energy of the resource payloads at release depends only on the ratio $\Omega$ between the centripetal and gravitational acceleration of a PM at the surface and the length of the chain normalized with respect to the asteroid radius. The parameter $\Omega$ can be expressed as [6]:

$$\Omega = \frac{\omega}{2\sqrt{\frac{G\pi\rho_A}{3}}} \tag{1}$$

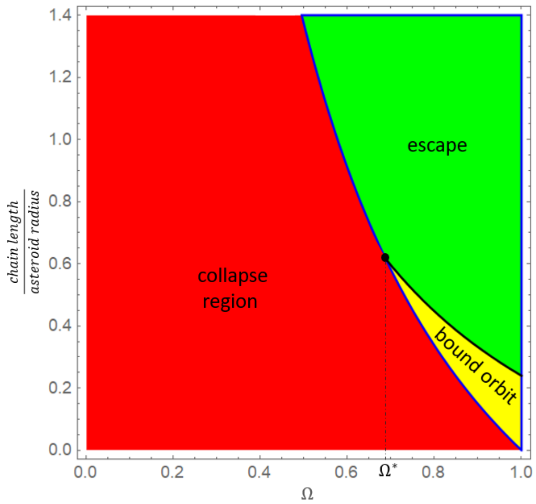


**Figure 2:** Regions of allowed (blue box) and forbidden motion (red region) for the orbital siphon. Adapted from [6].

where $\omega$ is the angular velocity of the asteroid, $G = 6.67 \times 10^{-11}\,\mathrm{m^3\,kg^{-1}\,s^{-2}}$ is the gravitational constant and $\rho_A$ is the density of the asteroid.

Figure 2 shows the region where the specific energy of the PM at release is negative (yellow region) and positive (green region). Any chain operating within the yellow region will release material into a bound orbit around the asteroid, whereas material is sent to escape if the chain operates in the green region. The red area is associated with a collapsing chain, where the orbital siphon effect cannot take place.

In this paper the negative energy region is of interest. In fact, the released material can be stored in orbit and then collected by an orbiting spacecraft for processing. The large surface-to-volume ratio of the released resources would enable more efficient water/metal extraction by sublimation, using solar concentrator technologies.

It is apparent from Fig. 2 that the condition $\Omega > \Omega^* = 0.687$ [6] must be verified for releasing material into bound motion, thus limiting asteroids suitable for this application. If $\Omega < \Omega^*$ the minimum length of the chain of masses required for the orbital siphon to operate is large enough to deliver material into escape. Then, from Eq. (1), suitable candidates are fast rotators with low density.

Possible candidates selected from the *Asteroid Lightcurve Database* [7] are shown in Table 1, where the required chain length and extractable mass are indicated (for details on how to evaluate these parameters the reader is referred to [6]). An estimate of the extractable water is also indicated, assuming that the water content of the asteroid is $0.15\%$ of its mass (this value is an estimate for $S$-type asteroids taken from [8]) and that the efficiency of the process is $50\%$. A reference den-

**Table 1:** Physical characteristics of candidate asteroids for disassembly using the orbital siphon effect. Required chain length, maximum extractable mass and an estimate of the extractable water are indicated for each candidate.

| Asteroid | Class | Radius [m] | Period [hours] | $\Omega$ | Chain Length [m] | Extractable mass [kg] | Extractable water (estimate) [kg] |
|---|---|---|---|---|---|---|---|
| 2002 EZ11 | S | 254 | 2.33 | 0.864 | 94 | 6.89E+09 | 5.17E+06 |
| 2004 VW14 | S | 196 | 2.50 | 0.804 | 87 | 2.86E+09 | 2.14E+06 |
| 2002 OA22 | S | 196 | 2.62 | 0.767 | 97 | 2.67E+09 | 2.01E+06 |
| 2008 CL1 | S | 187 | 2.62 | 0.766 | 92 | 2.32E+09 | 1.74E+06 |
| 2012 TM139 | S | 171 | 2.68 | 0.750 | 88 | 1.71E+09 | 1.28E+06 |
| 2006 BN55 | S | 163 | 2.83 | 0.711 | 94 | 1.38E+09 | 1.04E+06 |
| 2002 SR41 | S | 142 | 2.28 | 0.880 | 50 | 1.25E+09 | 9.37E+05 |
| 2002 CQ11 | S | 149 | 2.61 | 0.771 | 72 | 1.17E+09 | 8.80E+05 |
| 2005 WK4 | S | 142 | 2.60 | 0.774 | 68 | 1.03E+09 | 7.73E+05 |
| 2005 TF | S | 136 | 2.57 | 0.782 | 64 | 9.08E+08 | 6.81E+05 |
| 2010 TC55 | S | 130 | 2.45 | 0.822 | 54 | 8.52E+08 | 6.39E+05 |
| 2014 SM143 | S | 130 | 2.91 | 0.691 | 79 | 6.65E+08 | 4.99E+05 |
| 2008 WM64 | S | 113 | 2.41 | 0.835 | 45 | 5.72E+08 | 4.29E+05 |
| 1999 AQ10 | S | 118 | 2.67 | 0.753 | 61 | 5.69E+08 | 4.26E+05 |
| 2001 YB5 | S | 98 | 2.50 | 0.804 | 43 | 3.58E+08 | 2.68E+05 |
| 2016 JC6 | S | 82 | 2.28 | 0.882 | 29 | 2.37E+08 | 1.78E+05 |
| 2004 BE86 | S | 80 | 2.42 | 0.830 | 33 | 2.04E+08 | 1.53E+05 |
| 2016 WJ1 | S | 82 | 2.68 | 0.750 | 42 | 1.86E+08 | 1.40E+05 |
| 2016 NG33 | S | 75 | 2.32 | 0.866 | 27 | 1.76E+08 | 1.32E+05 |
| 2010 AF30 | S | 68 | 2.60 | 0.773 | 33 | 1.13E+08 | 8.47E+04 |
| 1995 CR | S | 68 | 2.66 | 0.755 | 35 | 1.09E+08 | 8.20E+04 |
| 2013 TE6 | S | 65 | 2.46 | 0.817 | 28 | 1.07E+08 | 8.01E+04 |
| 2017 GM4 | S | 62 | 2.88 | 0.698 | 37 | 7.41E+07 | 5.56E+04 |
| 2010 RC130 | S | 54 | 2.89 | 0.695 | 33 | 4.87E+07 | 3.65E+04 |
| 2002 FD6 | S | 47 | 2.80 | 0.718 | 27 | 3.36E+07 | 2.52E+04 |
| 2014 SX261 | S | 47 | 2.80 | 0.717 | 27 | 3.35E+07 | 2.51E+04 |
| 2006 UA216 | S | 29 | 2.50 | 0.803 | 13 | 8.77E+06 | 6.58E+03 |
| 2015 FG36 | S | 27 | 2.32 | 0.866 | 10 | 8.37E+06 | 6.28E+03 |
| 2013 UH5 | S | 23 | 2.69 | 0.747 | 12 | 3.90E+06 | 2.93E+03 |
| 2003 SR84 | S | 12 | 2.35 | 0.854 | 5 | 7.19E+05 | 5.39E+02 |

sity of $\rho_A = 2700\,\mathrm{kg\,m^{-3}}$ [9] has been used to estimate the mass of the asteroids and $\Omega$. Among all the possible candidates with $\Omega > \Omega^*$ asteroids requiring chain length larger than 100 m are excluded from this list. As expected, all objects matching these requirements are fast rotators, with a rotation period shorter than 3 h.

### 3. System architecture concept

To guarantee proper operation of the orbital siphon, the chain of masses has to be constrained to maintain a radial path during the ascent. This can be achieved using a rigid or semi-rigid cantilever truss fixed at the surface of the asteroid [5]. However, a much simpler solution to maintain the chain of masses in a quasi-radial path can by achieved using a tether and ballast mechanism (Fig. 3). The tether is kept taut by an anchoring device at the surface and by a ballast at the top. The ballast, placed at a larger altitude than the PM release location, would provide tension to the tether due to the centripetal force associated with the asteroid rotation. The tether length and ballast mass can be designed such that the center of mass is above synchronous orbit to support the whole system.

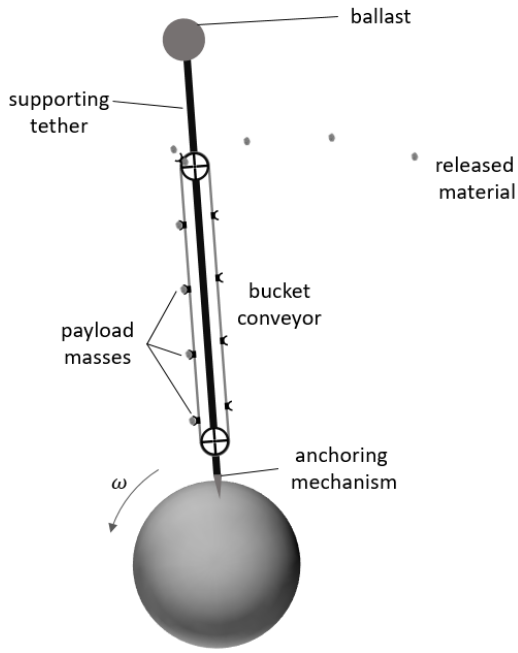


**Figure 3:** Proposed system architecture to maintain a quasi-radial stream of resource payloads into orbit using a tether and ballast mass as support structure.

The initial mass for the ballast can be provided by the spacecraft spooling the tether. Additional mass may be provided using the extracted resources. In this preliminary analysis, the ballast mass is taken within a range from 500 kg to 2500 kg.

A major constraint in this scenario is the max-

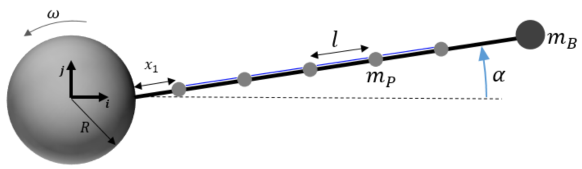


**Figure 4:** Model for the tether and ballast system, with bucket conveyor.

imum force available from the anchoring mechanism, which will depend on the surface properties of the asteroid (which are generally unknown [10]) and the design of the anchoring system. Liu et al. [11] conducted experiments to estimate the anchoring force provided by a conical anchor tip in sand and soil. They found forces ranging from 10 N to 385 N for soil and from 18 N to 26 N for an interval of penetrating depths from approximately 100 mm to 350 mm. Use of multiple anchoring tips could increase this force, however, for the preliminary analysis in this paper, it is assumed that the maximum force available at the surface is $f_{max} = 26$ N.

As for the chain, a possible solution to provide a continuous stream of mass into orbit is a bucket conveyor mechanism (Fig. 3). Assuming negligible friction, the bucket would work as a chain of masses and would be powered by the reaction centripetal pull on the payloads, as described in the previous section. A major advantage of a bucket conveyor is that the payloads do not have to slide along the tether, as the conveyor is disconnected from the supporting tether. This would eliminate the wear on the tether due to the continuous sliding of the PMs.

Material is assumed to be collected by rovers operating on the surface and then attached to the bucket conveyor. Released material would then orbit around the asteroid. An orbiting spacecraft is envisaged to collect material for processing.

The efficiency of this system is clearly related to the maximum mass flow rate obtainable from the bucket conveyor, by keeping the oscillation of the system small and the anchoring force below $f_{max}$.

#### 4. Model

Assuming that the radius of the pulleys in the bucket mechanism is small with respect to the conveyor length, that the mass of the bucket conveyor is negligible with respect to the mass of the payloads and neglecting any friction, the entire system can effectively be modelled as represented in Fig. 4. It is also assumed that the distance $l$ between consecutive PMs in the bucket conveyor is constant. The total length of the conveyor is therefore $L_C = (n-1)l$.

Let $x_i$ be the distance of the $i$-th PM from the anchoring point. Then

$$x_i = x_1 + (i-1)l. \tag{2}$$

Likewise, the coordinate $s$ defines the distance of a point on the tether with respect to the anchoring point. A reference frame with origin at the centre of the asteroid is defined by the unit vectors $\mathbf{i}$ and $\mathbf{j}$ in the asteroid equatorial plane, with $\mathbf{i}$ oriented along the radial direction. The unit vector $\mathbf{k}$ completes the triad and is parallel to the angular velocity vector. This reference frame is rotating with constant angular velocity $\omega\mathbf{k}$ with respect to an inertial frame. The tether can rotate in the plane defined by $\mathbf{i}$ and $\mathbf{j}$. Let $\alpha$ be the angle formed by the tether and the local vertical.

The variation of asteroid mass, radius and angular velocity due to mass extraction are neglected here for simplicity.

The position vector for the i-th PM, the tether and the ballast can then be written as, respectively:

$$\mathbf{r_{Pi}} = (R + x_i\cos\alpha)\mathbf{i} + (x_i\sin\alpha)\mathbf{j} \tag{3a}$$

$$\mathbf{r_T}(s) = (R + s\cos\alpha)\mathbf{i} + (s\sin\alpha)\mathbf{j} \tag{3b}$$

$$\mathbf{r_B} = (R + L_T\cos\alpha)\mathbf{i} + (L_T\sin\alpha)\mathbf{j} \tag{3c}$$

where $R$ is the asteroid radius and $L_T$ is the length of the tether. The velocity vectors are then:

$$\begin{aligned}\mathbf{v_{Pi}} &= \omega\hat{k} + \dot{\mathbf{r}}_{Pi} = \\ &= [\dot{x}_1\cos\alpha - (\omega+\dot{\alpha})x_i\sin\alpha]\,\mathbf{i} + \\ &+ [\omega R + \dot{x}_1\sin\alpha + (\omega+\dot{\alpha})x_i]\,\mathbf{j}\end{aligned} \tag{4a}$$

$$\begin{aligned}\mathbf{v}_T(s) &= -[(\omega+\dot{\alpha})s\sin\alpha]\,\mathbf{i} + \\ &+ [(\omega+\dot{\alpha})s\cos\alpha + \omega R]\,\mathbf{j}\end{aligned} \tag{4b}$$

$$\begin{aligned}\mathbf{v}_B &= -[(\omega+\dot{\alpha})L_T\sin\alpha]\,\mathbf{i} + \\ &+ [(\omega+\dot{\alpha})L_T\cos\alpha + \omega R]\,\mathbf{j}\end{aligned} \tag{4c}$$

where the dot notation represents a derivative with respect to time. The total kinetic energy $K$ of the system can be written as

$$K = K_T + K_P + K_B \tag{5}$$

where $K_T$, $K_P$ and $K_B$ are the kinetic energy of the tether, PMs and ballast respectively:

$$K_P = \frac{1}{2}m_P\sum_{i=1}^{n}(\mathbf{v}_{Pi}\cdot\mathbf{v}_{Pi}) \tag{6}$$

$$K_T = \int_0^{L_T} A(s)\rho_T\,(\mathbf{v}_{Pi}\cdot\mathbf{v}_{Pi})\,ds \tag{7}$$

$$K_B = \frac{1}{2}m_B(\mathbf{v}_B\cdot\mathbf{v}_B) \tag{8}$$

Here $\rho_T$ and $A(s)$ are the tether mass density and cross section respectively. The total potential energy of the system is

$$U = U_P + U_T + U_B \tag{9}$$

where

$$U_P = -\sum_{i=1}^{n} \frac{\mu m_P}{\sqrt{\mathbf{r}_{Pi} \cdot \mathbf{r}_{Pi}}} \tag{10}$$

$$U_T = -\mu \int_0^{L_T} \frac{\rho_T A(s)}{\sqrt{\mathbf{r}_T(s) \cdot \mathbf{r}_T(s)}} \tag{11}$$

$$U_B = -\frac{\mu m_B}{\sqrt{\mathbf{r}_B \cdot \mathbf{r}_B}} \tag{12}$$

being $\mu = \frac{4}{3} G \rho_A \pi R^3$ is the gravitational parameter of the asteroid. Then, Lagrange's equations of motion for the two generalized coordinates $q_1 = x_1$ and $q_2 = \alpha$ can be written as

$$\frac{d}{dt}\frac{\partial K}{\partial \dot{q_k}} - \frac{\partial K}{\partial q_k} + \frac{\partial U}{\partial q_k} = 0 \tag{13}$$

By substituting Eqs. (5) and (9) into Eq. (13), assuming $\alpha \approx 0$ (this assumption will be validated later) and a tether with constant cross section, the equations of motion become:

$$n\ddot{x}_1 = \sum_{i=1}^{n} \left[ R\omega^2 + (\omega + \dot{\alpha})^2 x_i - \frac{\mu}{(R + x_i)^2} \right] \tag{14a}$$

$$\mathcal{M}\ddot{\alpha} + \mathcal{C}\dot{\alpha} + \mathcal{K}\alpha = \mathcal{T} \tag{14b}$$

where

$$\mathcal{M} = m_B L_T^2 + m_P \sum_{i=1}^{n} x_i^2 + \frac{1}{3} m_T L_T^2 \tag{15a}$$

$$\mathcal{C} = 2 m_P \dot{x}_1 \sum_{i=1}^{n} x_i \tag{15b}$$

$$\begin{aligned} \mathcal{K} = & \left( m_B L_T + m_P \sum_{i=1}^{n} x_i + \frac{1}{2} m_T L_T \right) R\omega^2 + \\ & - \frac{1}{2}\mu \frac{m_T}{R + L_T} + \\ & - \mu m_B \frac{L_T R}{(R + L_T)^3} - \mu m_P R \sum_{i=1}^{n} \frac{x_i}{(R + x_i)^3} \end{aligned} \tag{15c}$$

$$\mathcal{T} = -\mathcal{C}\omega \tag{15d}$$

and $m_T = \rho_T A L_T$ is the mass of the tether. Equation (14a) is similar to the equation of motion obtained in [6] for a chain of masses constrained to the radial direction but here the centripetal acceleration (i.e., the first term in the sum) is coupled with the tether motion via $\dot{\alpha}$. The term $\mathcal{M}$ in Eq. (14b) contains the equivalent inertia of the system, $\mathcal{C}$ is a damping term, associated with the motion of the chain, $\mathcal{K}$ contains centrifugal and gravitational terms (note that the latter have been linearised with respect to $\alpha$ by assuming $\alpha \approx 0$) and $\mathcal{T}$ is the torque acting on the tether due to the Coriolis force exerted by the chain. Each term defined by Eqs. (15) is time dependent, as both $x_1$ and $\dot{x}_1$ are function of time. However, as will be shown later, $\dot{x}_1$ can be considered constant after an initial transient phase. Moreover, the chain operates with $x_1 \in [0, l]$ and $l$ is usually small when compared to $L_C$ (e.g., in the case of a 100 m conveyor lifting 50 PMs, $l$ is approximately 2 m). Therefore, the coefficients appearing in Eq. (14b) can be approximated as constants by assuming $\dot{x}_1 = const = v_1$ and $x_1 = const = l/2$. The velocity $v_1$ is a reference velocity for the chain at the steady state, which will be discussed later. Let $\bar{\mathcal{M}}$, $\bar{\mathcal{C}}$, $\bar{\mathcal{K}}$, $\bar{\mathcal{T}}$ be constant coefficients in this scenario. Then, Eq. (14b) is decoupled from Eq. (14a) and can be rewritten in the form of a damped, forced harmonic oscillator

$$\ddot{\alpha} + 2\zeta W \dot{\alpha} + W^2 = \bar{\mathcal{T}}/\bar{\mathcal{M}} \tag{16}$$

where $\zeta = \bar{\mathcal{C}}/(2\sqrt{\bar{\mathcal{M}}\bar{\mathcal{K}}})$ is the damping ratio and $W = \sqrt{\bar{\mathcal{K}}/\bar{\mathcal{M}}}$ is the undamped angular frequency of the oscillator. Equation (16) admits a closed-form solution:

$$\alpha = \alpha_0 + S e^{-\zeta W t} \sin\left[\sqrt{1 - \zeta^2} W t + \phi\right] \tag{17}$$

where the constants $S$ and $\phi$ are found based on the initial conditions $\alpha(0)$ and $\dot{\alpha}(0)$. The angle

$$\alpha_0 = \frac{\bar{\mathcal{T}}}{\bar{\mathcal{K}}} \tag{18}$$

represents the *equilibrium angle* of the tether. Since $\bar{\mathcal{C}} > 0$ (14b), the tether will exponentially reduce its oscillation amplitude until eventually reaching equilibrium at $\alpha_0$. The time constant

$$\tau = \frac{1}{W\zeta} = 2\frac{\bar{\mathcal{M}}}{\bar{\mathcal{C}}} \tag{19}$$

represents the time required to reduce the oscillation amplitude by a factor $e$.

If $m_T \ll m_B$ and $L_C \ll L_T$ then

$$\alpha_0 \propto \frac{1}{L_T}\frac{m_P}{m_B} \tag{20a}$$

$$\tau \propto L_T \frac{m_B}{m_P} \tag{20b}$$

$$W \propto \sqrt{\frac{1}{L_T}} \tag{20c}$$

Then, tuning the parameters $L_T$, $m_P$, $m_B$ to decrease the equilibrium angle will in turn increase the time constant. Moreover, the natural angular frequency of oscillation decreases for longer tethers.

Note that, in theory, the chain could be designed to work with larger $\alpha_0$. However, if the chain is to be braked, the tether would then swing around the local vertical. Then, the amplitude of the resulting oscillation would be $2\alpha_0$ and the motion undamped ($\bar{\mathcal{C}} = 0$ if $\dot{x}_1 = 0$). If $\alpha_0$ is large, the resulting amplitude of the oscillations would be unacceptably large. For this reason it is advisable to keep the equilibrium angle small.

#### 4.1. Anchoring force and tether tension

Proper siphon operation requires a taut tether and a braking mechanism in case the chain of masses has to be slowed during operation. The anchoring device has to withstand the required forces, without exceeding $f_{max}$ (Sect. 3). A method to estimate these parameters is given in this section, under the assumption that $\alpha \approx 0$.

#### 4.1.1. Anchoring force

The net force $df_T$ acting on a length of tether $ds$ at distance $s$ from the surface is the sum of the centripetal and gravitational forces acting on that element such that

$$df_T = \rho_T A ds \left(\omega^2(R+s) - \frac{\mu}{(R+s)^2}\right) ds \quad (21)$$

Similarly, the net force necessary to keep the ballast mass at distance $L_T$ is

$$f_C = m_C \left(\omega^2(R+L_T) - \frac{\mu}{(R+L_T)^2}\right) \quad (22)$$

Therefore, the total anchoring force required to keep the tether and the ballast mass in position is

$$\begin{aligned} f_{TB} &= \left(\int_0^{L_T} df_T\right) + f_C \\ &= m_T \left[\frac{1}{2}\omega^2(L_T+2R) - \mu\frac{1}{R(R+L_T)}\right] + \\ &+ m_B \left[\omega^2(R+L_T) - \frac{\mu}{(R+L_T)^2}\right] \end{aligned} \quad (23)$$

If $m_T \ll m_B$ and $L_T$ is sufficiently large to neglect the gravitational force on the ballast mass then

$$f_{TB} \approx \omega^2 m_B (R+L_T) \quad (24)$$

The force required to brake the chain $f_C$ is the sum of centripetal and gravitational force acting on each PM. From [6]:

$$\begin{aligned} f_C &= \left(\frac{R}{l}\right)^2 \left[\Psi^{(1)}\left(\frac{R}{l}+n\right) - \Psi^{(1)}\left(\frac{R}{l}\right)\right] + \\ &+ \omega^2 n \left[1 + \frac{1}{2}\frac{R}{l}(n-1)\right]. \end{aligned} \quad (25)$$

where $\Psi^{(1)}$ is the polygamma function of order $1$ [12]. Therefore, the overall force in the $\mathbf{i}$ direction necessary for proper siphon operation is given by $f_{TB}$ when the bucket conveyor is moving and $f_{TB} + f_C$ if the conveyor belt is stationary.

The anchoring mechanism should also withstand a force $f_\perp$ in the $\mathbf{j}$ direction, due to the Coriolis force generated by the PMs on the tether:

$$f_\perp = 2n\omega m_P \dot{x}_1. \quad (26)$$

Therefore, the total force required by the anchoring mechanism must verify the following constraint:

$$\sqrt{(f_{TB}+f_C)^2 + f_\perp^2} \leq f_{max}. \quad (27)$$

#### 4.1.2. Tether maximum tension

The equation for the tension $\sigma$ along the tether can be found substituting $df_T = d\sigma A$ in Eq. (21)

$$\frac{d\sigma}{ds} = \rho_T ds \left(\omega^2(R+s) - \frac{\mu}{(R+s)^2}\right) \quad (28)$$

When $s = s_{sync} = (\mu/\omega^2)^{1/3} - R$ then $d\sigma/ds = 0$. Since $d^2\sigma/ds^2 < 0$, the tension is maximum at $s = s_{sync}$, regardless of the boundary condition at the extremes of the tether. Integrating Eq. (28) from $s = 0$ to $s = s_{sync}$ subject to initial condition $\sigma(s = 0) = f_{TB}/A$ permits the maximum tension on the tether to be found as:

$$\sigma_{max} = \mu\rho_T \left(\frac{1}{R} + \frac{1}{2}\frac{R^2}{R_s^3} - \frac{3}{2}\frac{1}{R_s^3}\right) + \frac{f_{TB}}{A} \quad (29)$$

where $R_s = R + s_{sync}$. The maximum tension $\sigma_{max}$ must be smaller than the maximum tensile strength for the selected tether material.

### 5. Results

Equations (14) can be numerically integrated for a given set of initial conditions $x_1(0)$ , $\dot{x}_1(0)$, $\alpha(0)$ and $\dot{\alpha}(0)$. When $x_1 = l$ a new PM is connected to the chain while the top payload is removed. To evaluate the new chain velocity $\dot{x}_1^{new}$ each time a new PM is attached to the chain, conservation of linear momentum can be used. In particular, it can be shown that the new chain velocity can be calculated from the velocity at the previous step $\dot{x}_1^{old}$:

$$\dot{x}_1^{new} = \frac{n-1}{n}\dot{x}_1^{old}. \quad (30)$$

Equation (30) does not take into account the rigidity of the elements connecting PMs in the conveyor. However, for the purpose of this preliminary analysis, it represents a reasonable approximation.

Results presented in the following section are referred to the candidate asteroid 2002 EZ11 (Table 1). A bucket conveyor with $n = 50$ and total length $L_C = 94$ m is considered. Such a length guarantees that the maximum extractable mass is delivered into a bound orbit.

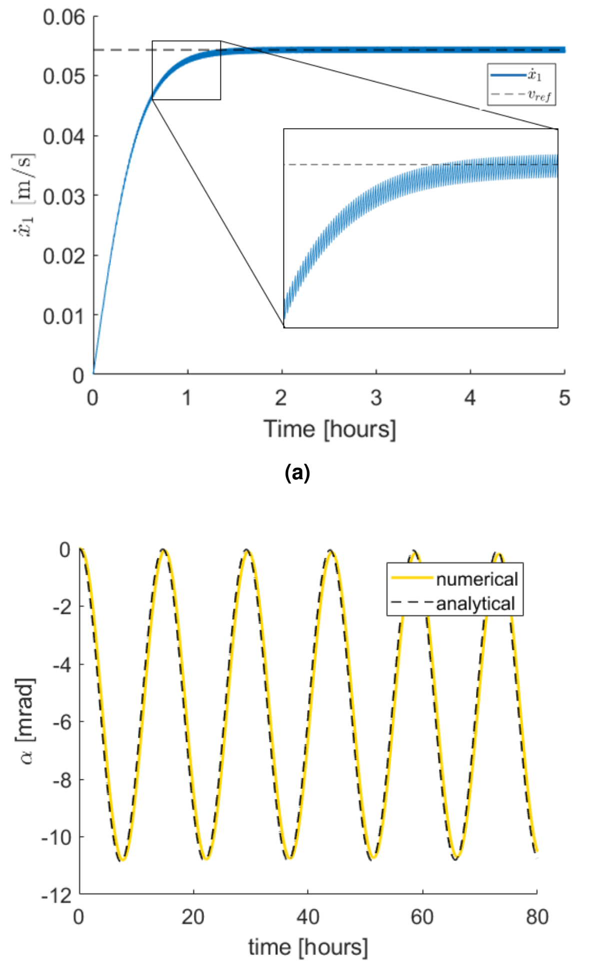


**Figure 5:** Chain velocity (continuous line) $\dot{x}_1$ as a function of time (a) and tether libration as a function of time (b) The dotted line in (a) represents the reference velocity (Eq. (31)).

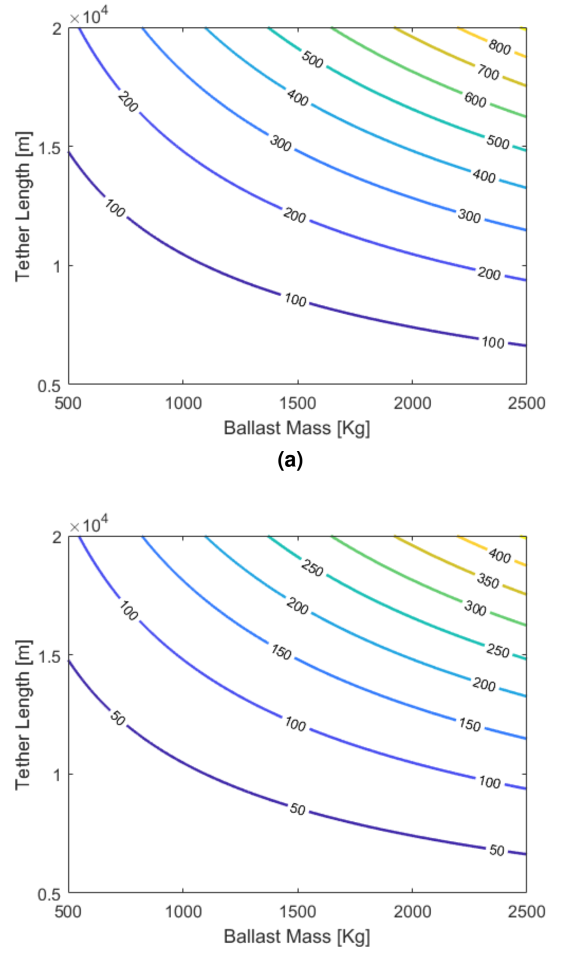


**Figure 6:** Time constant (in days) as a function of $m_B$ and $L$ for $m_P = 50$ kg (top) and $m_P = 100$ kg (bottom).

### 5.1. Chain velocity and libration angle

Figure 5 shows the chain velocity (continuous line) as a function of time, assuming the initial conditions $x(0) = 0$, $\dot{x}_1(0) = 0$, $\alpha(0) = 0$ and $\dot{\alpha}(0)$ = 0. For this simulation a Spectra 2000 tether with cross section $A = 0.5\,\text{mm}^2$ (density and maximum tensile strength are listed in Table 2) is chosen. The ballast mass is $m_B = 1500$ kg. Each time a new PM is attached to the chain, $\dot{x}_1$ changes according to Eq. (30). After an initial transient, the chain velocity oscillates between a minimum and maximum. The maximum velocity is reached every time $x_1 = l$. When a new payload is attached to the chain, the velocity slightly decreases, following Eq. (30). The black dashed line represents the velocity $v_{ref}$ of a chain with length $L_C$ under the assumption $n \to \infty$ [6] such that:

$$v_{ref} = \sqrt{\frac{1}{2}\frac{L_C}{R}\left(2 + \frac{L_C}{R} - \frac{2}{(1 + L_C/R)\Omega^2}\right)}. \quad (31)$$

It is apparent from Fig. 5 that $v_{ref}$ is a reasonable approximation of $\dot{x}_1$ at the steady state.

Figure **??** shows the angle $\alpha$ with respect to the time, solving Eq. (14b) (continuous line) and Eq. (16) (dotted line). Equation (16) admits the analytical solution given by Eq. (17). The chain reference velocity to be used in Eq. (16) has been set to $v_{ref}$ (Eq. (31)). With the convention adopted in Fig. 4 the oscillation angle $\alpha$ is negative. The two solutions provide basically identical results. Similar behaviour is observed by varying the tether and chain parameters. Therefore, Eq. (16) can be regarded as a valid approximation of the tether dynamics and can be exploited for further analysis.

### 5.2. Time constant and equilibrium angle

Figure 6 shows the variation of the time constant $\tau$ as a function of $m_B$ and $L_T$, for $m_P = 50$ kg (a) and $m_P = 100$ kg (b). The time constant is generally large ($\approx 10^2$ - $10^3$ days), i.e., the tether takes a significant amount of time to reduce its oscillation amplitude. Note that the two contours are qualitatively the same, only rescaled by a factor $2$.

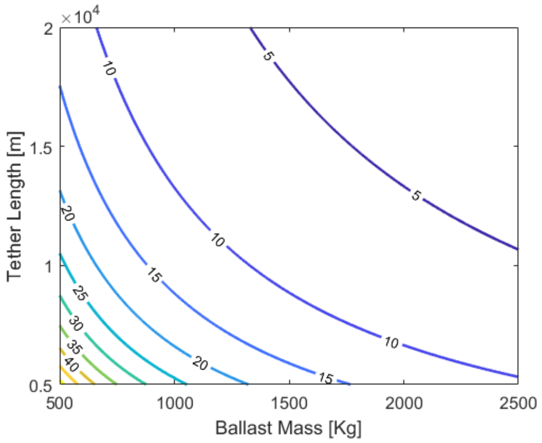


**(a)**

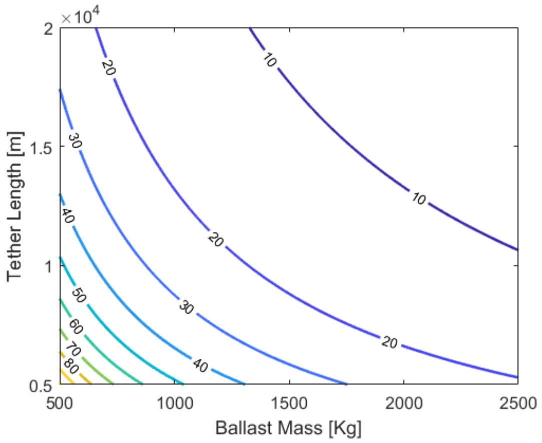


**(b)**

**Figure 7:** Equilibrium angle (absolute value in milliradians) as a function of $m_B$ and $L$ for $m_P = 50$ kg (a) and $m_P = 100$ kg (b).

In fact, for a Spectra 2000 tether with cross section $A = 0.5$ mm$^2$, the tether mass is three order of magnitude smaller with resepct to the ballast mass for the range of $L_T$ chosen and $L_C \ll L_T$. For this reason, the hypotheses of Eqs. (20) are verified and $\tau$ is inversely proportional to $m_P$.

Figure Fig. 7 shows the absolute value of $\alpha_0$ with respect to $L_T$ and $m_B$, again for $m_P = 50$ kg (a) and $m_P = 100$ kg (b). In this case, $\alpha_0$ increase for larger $m_B$, $L_T$ and smaller $m_P$.

Therefore, the choice of the parameters $m_P$, $m_B$, and $L_T$ must be a trade-off between the desired time constant and the equilibrium angle. For the selected range of $L_T$ and $m_B$, $\alpha_0$ is small, below 80 mrad and hence the conveyor is almost vertical.

### 5.3. Tether material

Table 2 shows the effects of selecting different tether materials and cross-sections on the equilibrium angle $\alpha_0$, the tether mass $m_T$, the maximum tension on the tether $\sigma_{max}$ and the required anchoring radial forces $f_T$, $f_B$ ($f_C$ and $f_\perp$ are not listed here as they do not depend on the characteristics of the tether), assuming $L = 10\,000$ m, $m_P = 50$ kg and $m_B = 1500$ kg. Several points can be deduced.

**Table 2:** Density and maximum tensile strength for some materials.

| Material | Density [Kg/m$^3$] | Max tensile strength [GPa] |
|---|---|---|
| Spectra 2000 | 970 | 3.25 |
| Carbon nanotubes | 1300 | 130 |
| Kevlar | 1440 | 3.6 |
| Steel | 7900 | 5 |

**Table 3:** Effect of the material density on the equilibrium angle, tether mass, maximum tension along the tether and anchoring force.

| Material | A mm$^2$ | $\alpha_0$ mrad | $m_T$ kg | $\sigma_{max}$ MPa | $f_T$ N | $f_B$ N |
|---|---|---|---|---|---|---|
| Spectra 2000 | 0.5 | 4.9 | 4.9 | 17.3 | 0.01 | 8.7 |
| | 5 | 4.5 | 48.5 | 1.8 | 0.14 | 8.7 |
| Carbon nanotubes | 0.5 | 4.6 | 6.5 | 17.3 | 0.02 | 8.7 |
| | 5 | 4.4 | 65 | 1.8 | 0.19 | 8.7 |
| Kevlar | 0.5 | 4.5 | 7.2 | 17.3 | 0.02 | 8.7 |
| | 5 | 4.5 | 72 | 1.8 | 0.21 | 8.7 |
| Steel | 0.5 | 4.5 | 39.5 | 17.5 | 0.11 | 8.7 |
| | 5 | 4.0 | 395 | 1.9 | 1.16 | 8.7 |

- The decrease in $\alpha_0$ using denser material is negligible.
- Larger cross sections, which would increase the mass of the tether, do not significantly reduce $\alpha_0$.
- The maximum tension on the tether is always (several order of magnitude) smaller than the maximum tensile strength for the material.
- The anchoring force is virtually independent of the tether characteristics. In fact, the tether masses are 2 to 3 orders of magnitude smaller than the mass of the ballast, therefore $f_T$ is negligible with respect to $f_B$ (Eq. (24)).

For these reasons, the choice of material does not have significant consequences on the dynamics. In particular, the inertia of the tether does not significantly contribute to reducing the equilibrium angle. Thus, minimization of mass would be the main driver influencing the selection. In this case, a Spectra 2000 tether with cross section of 0.5 mm$^2$ is the best choice among the proposed materials.

### 5.4. Mass flow rate

Table 4 shows the required tether length, tether mass and anchoring force to maintain a given

**Table 4:** Tether length, tension and anchoring force requirements for several mass flow rates $\dot{m}_P$.

| $\dot{m}_P$ [kg/s] | $L_T$ [km] | $m_T$ [kg] | $\sigma_{max}$ [MPa] | $f_{TB}$ [N] | $f_C$ [N] | $f_\perp$ [N] |
|---|---|---|---|---|---|---|
| 1 | 1.2 | 0.6 | 2.5 | 1.3 | 0.1 | 0.1 |
| 5 | 6.2 | 3.1 | 10.9 | 5.5 | 0.3 | 0.7 |
| 10 | 12.5 | 6.1 | 21.5 | 10.8 | 0.5 | 1.4 |
| 20 | 24.8 | 12.2 | 42.6 | 21.3 | 0.8 | 2.8 |

mass flow rate $\dot{m}_P$ using a ballast mass $m_B = 1500\,\text{kg}$ such that $\alpha_0 = 25\,\text{mrad}$. The mass flow rate is evaluated considering the time between two subsequent releases of PMs, i.e., $l/v_{ref}$ (assuming $\dot{x}_1 = const = v_{ref}$).

Note that, for an asteroid with given $\Omega$ and $R$, the radial velocity of the conveyor $v_{ref}$ (Eq. (31)) only depends on the length of the conveyor $L_C$. Therefore, if $L_C$ is fixed, the only way to increase the mass flow rate is by using larger payload masses. Then, to keep $\alpha_0$ constant (with constant $m_B$), longer tethers must be used (Eq. (20a)). The maximum tether tension is below $1\,\text{MPa}$ for $\dot{m}_P < 20\,\text{kg}\,\text{s}^{-1}$, several order of magnitude below the maximum tensile strength for Spectra 2000. For $\dot{m}_P < 20\,\text{kg}\,\text{s}^{-1}$ the required anchoring force always satisfies Eq. (27). It should be noted, however, that the major component in the anchoring force is due to $f_{TB}$. The braking force $f_C$ and the transversal force $f_\perp$ are always negligible with respect to $f_{TB}$.

### 6. Further improvements

It has been noted that, if the chain has to be braked, the tether will oscillate along the local vertical with amplitude $2\alpha_0$ and this oscillation might be anyway unwanted. Possible methods to reduce this oscillation are proposed.

- The conveyor could be activated every time the tether is swinging with $\dot{\alpha} > 0$. The Coriolis forces would produce a "braking" torque which could help minimizing the oscillation.
- The required torque to reduce the oscillation could be provided by a thruster positioned on the counterweight.

In particular, the second method could also help to decrease the time constant $\tau$ and thus reducing the oscillation about $\alpha_0$ while the conveyor is in operation. These methods may be considered for future analysis.

Clearly, the results found in this paper only provide a general overview on the feasibility of the concept. Moreover, the variation of asteroid mass, radius and angular velocity were not included in this simple model. Clearly, future developments should include this and several additional factors. In particular: accurate design of the bucket conveyor, effects of non-spherical gravitational field, surface mining techniques and resource processing technologies.

### 7. Conclusions

The orbital siphon concept represents an efficient means to raise resource payloads from the surface of an asteroid without the need for external work to be done. At the core of this concept is to leverage the rotational kinetic energy of the asteroid to lift a vertical chain of tether-connected resource payloads. Candidate asteroids matching the requirements to raise material in a bound orbit are listed.

The orbital siphon concept can be applied for asteroid disassembly. Resources with large surface-to-volume ratio would be delivered to a bound orbit around the asteroid and then processed using solar thermal concentrators.

It is proposed that such a chain of resource payloads could be realized using a conveyor mechanism. The conveyor is connected to a tether and ballast, supporting the whole system.

Engineering requirements for such a resource extraction system have been discussed. In particular, tension requirements for the tether are not restrictive. Spectra 2000 has been proposed as a candidate material for its low density.

It has been shown that tether oscillation during operation are generally small and the anchoring force requirements are compatible with the maximum force provided by a conical anchor tip in loose soil. It is shown that, using a ballast mass of $1500\,\text{kg}$ a stream of resources up to $20\,\text{kg}\,\text{s}^{-1}$ can be sent into orbit around a candidate asteroid for processing.

**Acknowledgements.** AV acknowledges a College of Science and Engineering Scholarship and CM acknowledges support from a Royal Society Wolfson Research Merit Award.

### References

[1] S. D. Ross. Near-earth asteroid mining. *Space Industry Report, Caltech, Pasadena*, 2001. `http://space.nss.org/media/Near-Earth-Asteroid-Mining-Ross-2001.pdf`.

[2] C. McInnes. Harvesting Near Earth Asteroid Resources Using Solar Sail Technology. *4th International Symposium on Solar Sailing (ISSS 2017)*.

[3] K. Zacny, M. Cohen, W. James, and B. Hilscher. Asteroid Mining. *American Institute of Aeronautics and Astronautics*, 2013.

[4] J. W. McMahon. Dismantling rubble pile asteroids with AoES (area-of-effect soft-bots). `http://aiweb.techfak.uni-bielefeld.de/content/bworld-robot-control-software/`, 2018.

[5] C. McInnes and C. Davis. Novel payload dynamics on space elevators systems. *56th International Astronautical Congress (IAC-05-D4.2.07)*, 2005.

[6] A. Viale, C. R. McInnes, and M. Ceriotti. Analytical mechanics of asteroid disassembly using the orbital siphon concept (submitted). *Proceedings Royal Society A*.

[7] B. D. Warner, A. W. Harris, and P. Pravec. The asteroid lightcurve database. *Icarus*, 202(1):134–146, 2009 (Updated 2018 June 23). `http://www.MinorPlanet.info/lightcurvedatabase.html`.

[8] J. P. Sanchez and C. R. McInnes. Assessment on the feasibility of future shepherding of asteroid resources. *Acta Astronautica*, 73:49–66, 2012.

[9] E. M. Standish. Recommendation of DE405 for 2001 Mars Surveyor and for Cassini. *JPL Interoffice Memorandum*, 2000.

[10] K. Zacny, P. Chu, G. Paulsen, M. Hedlund, B. Mellerowicz, S. Indyk, J. Spring, A. Parness, D. Wegel, R. Mueller, and D. Levitt. Asteroids: Anchoring and sample acquisition approaches in support of science, exploration, and in-situ resource utilization. *Springer, Berlin, Heidelberg*, pages 287–343, 2013.

[11] H. Liu, Z. Zhao, and J. Zhao. Preliminary anchoring technology for landing on the asteroid. In *2013 IEEE International Conference on Robotics and Biomimetics (ROBIO)*, pages 2392–2396.

[12] M. Abramowitz and I. A. Stegun. *Handbook of mathematical functions: with formulas, graphs, and mathematical tables*, volume 55. Courier Corporation, 1964.